US007653260B2

(12) **United States Patent**
Perz et al.

(10) **Patent No.: US 7,653,260 B2**
(45) **Date of Patent: Jan. 26, 2010**

(54) **SYSTEM AND METHOD OF REGISTERING FIELD OF VIEW**

(75) Inventors: **Cynthia B. Perz**, Huntington Beach, CA (US); **Jose De La Torre-Bueno**, Carlsbad, CA (US)

(73) Assignee: **Carl Zeis MicroImaging GmbH**, Jena (DE)

(*) Notice: Subject to any disclaimer, the term of this patent is extended or adjusted under 35 U.S.C. 154(b) by 912 days.

(21) Appl. No.: **10/872,138**

(22) Filed: **Jun. 17, 2004**

(65) **Prior Publication Data**

US 2005/0281484 A1 Dec. 22, 2005

(51) **Int. Cl.**
G06K 9/36 (2006.01)

(52) **U.S. Cl.** **382/284**; 382/128; 382/133

(58) **Field of Classification Search** 382/284
See application file for complete search history.

(56) **References Cited**

U.S. PATENT DOCUMENTS

3,824,393	A	7/1974	Brain
3,851,972	A	12/1974	Smith et al.
4,011,004	A	3/1977	Levine et al.
4,125,828	A	11/1978	Resnick et al.
4,196,265	A	4/1980	Koprowski et al.
4,210,419	A	7/1980	Castleman
4,249,825	A	2/1981	Shapiro
4,338,024	A	7/1982	Bolz et al.
4,342,905	A	8/1982	Fujii et al.
4,349,528	A	9/1982	Koprowski et al.
4,364,932	A	12/1982	Kung et al.
4,364,933	A	12/1982	Kung et al.
4,364,934	A	12/1982	Kung et al.
4,364,935	A	12/1982	Kung et al.
4,364,936	A	12/1982	Kung et al.
4,364,937	A	12/1982	Kung et al.

(Continued)

FOREIGN PATENT DOCUMENTS

DE 3340647 5/1985

(Continued)

OTHER PUBLICATIONS

Arklie, et al., "Differentiation Antigens Expressed by Epithelial Cells in the Lactating Breast are also Detectable in Breast Cancers", *Int. J. Cancer*, vol. 28, pp. 23-29, 1981.

(Continued)

Primary Examiner—Sath V Perungavoor
(74) *Attorney, Agent, or Firm*—Patterson, Thuente, Skaar & Christensen, P.A.

(57) **ABSTRACT**

Disclosed is a system for and a method of registering images captured by a computer-controlled microscope. The imaging system of the present invention includes a computer-controlled microscope electrically connected to a controller having a display device. The microscope further includes a bar-code reader, a camera, a serial interface, one or more sensors, one or more motors, a light source, a turret, and a data interface. The method of image registration includes the steps of defining areas of interest on a microscope slide, creating a database of microscopic image locations, commanding a microscope to each location, capturing and storing an image, calculating correlation with neighbors, registering correlation scores and offsets, determining an anchor, and attaching neighbors using correlation scores and offsets.

22 Claims, 9 Drawing Sheets

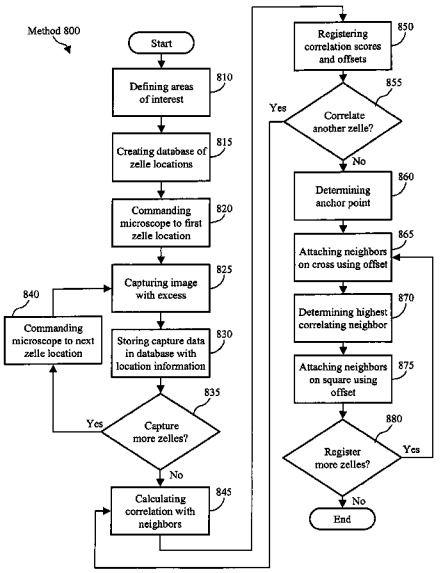

U.S. PATENT DOCUMENTS

4,393,466	A		7/1983	Deindorfer et al.	
4,513,438	A		4/1985	Graham et al.	
4,612,614	A		9/1986	Deindorfer et al.	
4,656,594	A		4/1987	Ledley	
4,673,973	A		6/1987	Ledley	
4,700,298	A		10/1987	Palcic et al.	
4,741,043	A		4/1988	Bacus et al.	
4,939,240	A		7/1990	Chu et al.	
4,945,220	A		7/1990	Mallory et al.	
4,965,725	A		10/1990	Rutenberg	
4,991,223	A		2/1991	Bradley	
5,003,165	A		3/1991	Sarfati et al.	
5,008,185	A		4/1991	Bacus	
5,016,173	A		5/1991	Kenet et al.	
5,018,209	A	*	5/1991	Bacus	382/129
5,051,816	A		9/1991	Harrison et al.	
5,068,909	A		11/1991	Rutherford et al.	
5,085,325	A		2/1992	Jones et al.	
5,086,477	A	*	2/1992	Yu et al.	382/145
5,087,965	A		2/1992	Torre-Bueno	
5,123,055	A		6/1992	Kasdan	
5,140,647	A	*	8/1992	Ise et al.	382/284
5,202,931	A		4/1993	Bacus	
5,218,645	A	*	6/1993	Bacus	382/133
5,231,580	A		7/1993	Cheung et al.	
5,233,684	A		8/1993	Ulichney	
5,235,522	A		8/1993	Bacus	
5,254,845	A		10/1993	Burgess et al.	
5,257,182	A	*	10/1993	Luck et al.	382/224
5,268,966	A	*	12/1993	Kasdan	382/133
5,287,272	A	*	2/1994	Rutenberg et al.	382/224
5,301,244	A	*	4/1994	Parulski	382/319
5,317,140	A		5/1994	Dunthorn	
5,321,545	A		6/1994	Bisconte	
5,333,207	A		7/1994	Rutenberg	
5,338,924	A		8/1994	Barrett et al.	
5,352,613	A		10/1994	Tafas et al.	
5,375,177	A		12/1994	Vaidyanathan et al.	
5,409,007	A		4/1995	Saunders et al.	
5,422,018	A		6/1995	Saunders et al.	
5,428,690	A		6/1995	Bacus et al.	
5,432,054	A		7/1995	Saunders et al.	
5,432,871	A		7/1995	Novik	
5,449,622	A		9/1995	Yabe et al.	
5,459,384	A		10/1995	Engelse et al.	
5,463,470	A		10/1995	Terashita et al.	
5,469,353	A		11/1995	Pinsky et al.	
5,473,706	A		12/1995	Bacus et al.	
5,481,401	A		1/1996	Kita et al.	
5,489,386	A		2/1996	Saunders	
5,499,097	A		3/1996	Ortyn et al.	
5,515,172	A		5/1996	Shiau	
5,526,258	A		6/1996	Bacus	
5,533,628	A		7/1996	Tao	
5,544,650	A		8/1996	Boon et al.	
5,546,323	A		8/1996	Bacus et al.	
5,561,611	A	*	10/1996	Avinash	702/111
5,583,666	A		12/1996	Ellson et al.	
5,585,469	A		12/1996	Kojima et al.	
5,586,160	A		12/1996	Mascio	
5,602,941	A		2/1997	Charles et al.	
5,610,022	A		3/1997	Battifora	
5,619,032	A	*	4/1997	Kasdan	250/201.3
5,625,705	A		4/1997	Recht	
5,625,709	A	*	4/1997	Kasdan	382/203
5,633,491	A	*	5/1997	Kasdan	250/201.3
5,635,402	A		6/1997	Alfano et al.	
5,644,139	A	*	7/1997	Allen et al.	250/557
5,646,677	A		7/1997	Reber et al.	
5,647,025	A	*	7/1997	Frost et al.	382/255
5,671,288	A	*	9/1997	Wilhelm et al.	382/128
5,686,960	A	*	11/1997	Sussman et al.	348/218.1
5,690,892	A		11/1997	Babler et al.	
5,691,779	A		11/1997	Yamashita et al.	
5,701,172	A		12/1997	Azzazy	
5,706,093	A		1/1998	Komiya	
5,726,009	A		3/1998	Conners et al.	
5,731,156	A		3/1998	Golbus	
5,735,387	A		4/1998	Polaniec et al.	
5,740,267	A		4/1998	Echerer et al.	
5,740,270	A	*	4/1998	Rutenberg et al.	382/133
5,773,459	A		6/1998	Tang et al.	
5,783,814	A		7/1998	Fairley et al.	
5,795,723	A		8/1998	Tapscott et al.	
5,796,861	A	*	8/1998	Vogt et al.	382/128
5,799,105	A		8/1998	Tao	
5,812,629	A	*	9/1998	Clauser	378/62
5,846,749	A		12/1998	Slamon et al.	
5,851,186	A		12/1998	Wood et al.	
5,854,851	A		12/1998	Bamberger et al.	
5,867,598	A		2/1999	De Queiroz	
5,877,161	A		3/1999	Riabowol	
5,880,473	A		3/1999	Ginestet	
5,888,742	A		3/1999	Lal et al.	
5,889,881	A		3/1999	MacAulay et al.	
5,911,003	A		6/1999	Sones	
5,911,327	A		6/1999	Tanaka et al.	
5,962,234	A		10/1999	Golbus	
5,966,309	A		10/1999	O'Bryan et al.	
5,966,465	A		10/1999	Keith et al.	
5,982,951	A	*	11/1999	Katayama et al.	382/284
6,005,681	A	*	12/1999	Pollard	358/473
6,006,191	A		12/1999	DiRienzo	
6,007,996	A		12/1999	McNamara et al.	
6,011,595	A		1/2000	Henderson et al.	
6,031,929	A		2/2000	Maitz et al.	
6,031,930	A	*	2/2000	Bacus et al.	382/133
6,040,139	A		3/2000	Bova	
6,058,322	A		5/2000	Nishikawa et al.	
6,069,242	A		5/2000	Zavada et al.	
6,072,570	A		6/2000	Chipman et al.	
6,087,134	A		7/2000	Saunders	
6,097,838	A		8/2000	Klassen et al.	
6,101,265	A	*	8/2000	Bacus et al.	382/133
6,117,985	A		9/2000	Thomas et al.	
6,122,017	A	*	9/2000	Taubman	348/620
6,122,400	A		9/2000	Reitmeier	
6,125,194	A		9/2000	Yeh et al.	
6,141,602	A		10/2000	Igarashi et al.	
6,151,535	A		11/2000	Ehlers	
6,160,618	A		12/2000	Garner	
6,169,816	B1		1/2001	Ravkin	
6,203,987	B1		3/2001	Friend et al.	
6,215,892	B1		4/2001	Douglass et al.	
6,215,894	B1	*	4/2001	Zeleny et al.	382/133
6,225,636	B1		5/2001	Ginestet	
6,226,392	B1	*	5/2001	Bacus et al.	382/128
6,226,636	B1		5/2001	Mottaleb et al.	
6,236,031	B1		5/2001	Ueda	
6,238,892	B1		5/2001	Mercken et al.	
6,255,465	B1		7/2001	Ferguson-Smith et al.	
6,259,807	B1		7/2001	Ravkin	
6,259,826	B1	*	7/2001	Pollard et al.	382/284
6,270,971	B1		8/2001	Ferguson-Smith et al.	
6,272,235	B1	*	8/2001	Bacus et al.	382/133
6,281,874	B1		8/2001	Sivan et al.	
6,290,907	B1		9/2001	Takahashi et al.	
6,313,452	B1		11/2001	Paragano et al.	
6,351,712	B1		2/2002	Stoughton et al.	
6,352,861	B1		3/2002	Copeland et al.	
6,374,989	B1		4/2002	Van Dyke, Jr. et al.	
6,379,929	B1		4/2002	Burns et al.	

6,396,941	B1 *	5/2002	Bacus et al.	382/128
6,404,906	B2 *	6/2002	Bacus et al.	382/128
6,418,236	B1 *	7/2002	Ellis et al.	382/128
6,466,690	B2	10/2002	Bacus et al.	
6,468,476	B1	10/2002	Friend et al.	
6,518,554	B1	2/2003	Zhang	
6,522,774	B1 *	2/2003	Bacus et al.	382/133
6,553,135	B1	4/2003	Douglass et al.	
6,606,413	B1 *	8/2003	Zeineh	382/232
6,625,332	B1 *	9/2003	Nakao	382/294
6,631,203	B2	10/2003	Ellis et al.	
6,647,151	B1 *	11/2003	Stallbaumer et al.	382/275
6,671,393	B2	12/2003	Hays et al.	
6,674,884	B2 *	1/2004	Bacus et al.	382/133
6,674,896	B1	1/2004	Torre-Bueno	
6,697,509	B2	2/2004	Torre-Bueno	
6,711,283	B1 *	3/2004	Soenksen	382/133
6,718,053	B1	4/2004	Ellis et al.	
6,775,402	B2 *	8/2004	Bacus et al.	382/133
7,027,628	B1 *	4/2006	Gagnon et al.	382/128
7,031,507	B2 *	4/2006	Bacus et al.	382/133
7,035,478	B2 *	4/2006	Crandall et al.	382/284
7,194,118	B1 *	3/2007	Harris et al.	382/128
7,253,420	B2 *	8/2007	Motomura	250/458.1
7,305,109	B1 *	12/2007	Gagnon et al.	382/128
2001/0050999	A1 *	12/2001	Bacus et al.	382/128
2002/0034762	A1	3/2002	Muller et al.	
2002/0061127	A1 *	5/2002	Bacus et al.	382/128
2002/0067409	A1	6/2002	Harari et al.	
2002/0164810	A1	11/2002	Dukor et al.	
2002/0181762	A1 *	12/2002	Silber	382/154
2002/0184605	A1 *	12/2002	Matsuoka	716/4
2003/0002718	A1 *	1/2003	Hamid	382/124
2003/0048931	A1 *	3/2003	Johnson et al.	382/128
2003/0123717	A1 *	7/2003	Bacus et al.	382/128
2003/0124589	A1	7/2003	Piper	
2003/0138140	A1	7/2003	Marcelpoil et al.	
2003/0170703	A1	9/2003	Piper et al.	
2004/0008894	A1 *	1/2004	Zeineh	382/240
2004/0136582	A1 *	7/2004	Bacus et al.	382/128
2004/0141637	A1 *	7/2004	Bacus et al.	382/128
2004/0252875	A1 *	12/2004	Crandall et al.	382/133
2005/0082494	A1 *	4/2005	Motomura	250/458.1
2005/0084175	A1 *	4/2005	Olszak	382/284
2005/0163398	A1 *	7/2005	Ioka	382/284
2005/0254696	A1 *	11/2005	Bacus et al.	382/128
2005/0281484	A1 *	12/2005	Perz et al.	382/294
2006/0034543	A1 *	2/2006	Bacus et al.	382/284
2006/0045388	A1 *	3/2006	Zeineh et al.	382/312
2006/0133657	A1 *	6/2006	Schmid et al.	382/128
2007/0019846	A1 *	1/2007	Bullitt et al.	382/128
2007/0036462	A1 *	2/2007	Crandall et al.	382/284
2007/0280517	A1 *	12/2007	De La Torre-Bueno et al.	382/128
2008/0032328	A1 *	2/2008	Cline et al.	435/40.5

FOREIGN PATENT DOCUMENTS

DE	3735091	4/1988
EP	0213666	3/1987
EP	0557871	9/1993
EP	0713086	5/1996
WO	WO 92/17848	10/1992
WO	WO 97/20198	6/1997
WO	WO 00/49391	8/2000
WO	WO 01/25476	4/2001
WO	WO 01/37206	5/2001
WO	WO 03/003057	1/2003
WO	WO 03/014795	2/2003
WO	WO 03/040064	5/2003

OTHER PUBLICATIONS

Atassi, "Precise Determination of Protein Antigenic Structures has Unravelled the Molecular Immune Recognition of Proteins and Provided a Prototype for Synthetic Mimicking of Other Protein Binding Sites", *Molecular & Cellular Biochemistry*, vol. 32, pp. 21-43, 1980.

Aziz, "Quantitation of Estrogen and Progesterone Receptors by Immunocytochemical and Image Analyses", *American Journal of Clinical Pathology*, vol. 98, No. 1, pp. 105-111, Jul. 1992.

Bacus, et al., "The Evaluation of Estrogen Receptor in Primary Breast Carcinoma by Computer-Assisted Image Analysis", *American Journal of Clinical Pathology*,vol. 90, No. 2, pp. 233-239, Aug. 1988.

Baddoura, et al., "Image Analysis for Quantitation of Estrogen Receptor in Formalin-Fixed Paraffin-Embedded Sections of Breast Carcinoma", *Modern Pathology*, vol. 4, No. 1, pp. 91-95, 1991.

Baer, et al., "Stochastic Models of Local Structures Versus Global Atomic Configurations", *Journal of Non-Crystalline Solids*, vols. 192 and 193, pp. 106-110, 1995.

Ballard, et al., *Computer Vision*, Prentice-Hall, Inc., Englewood Cliffs, New Jersey, USA, pp. 65-70; pp. 149-165, 1982.

Bander, "Monoclonal Antibodies to Renal Cancer Antigens", *European Urology*, vol. 18, No. 2, pp. 10-12, Aug. 1990.

Baxes, *Digital Image Processing Principles and Applications*, John Wiley & Sons, Inc., pp. 127-137.

Castleman, *Digital Image Processing*, Prentice Hall, Upper Saddle River, New Jersey, pp. 452-460; 551-554, 1996.

Caulet, et al., "Comparative Quantitative Study of Ki-67 Antibody Staining in 78B and T Cell Malignant Lymphoma (ML) Using Two Image Analyser Systems", *Path. Res. Pract.*, vol. 188, pp. 490-496, 1992.

Ceriani, et al., "Circulating human mammary epithelial antigens in breast cancer", *Proc. Natl. Acad. Sci.*, vol. 79, pp. 5420-5424, Sep. 1998.

Ceriani, et al., "Surface differentiation antigens of human mammary epithelial cells carried on the human milk fat globule", *Proc. Natl. Acad. Sci.*, vol. 74, No. 2, pp. 582-586, Feb. 1977.

ChromaVision, "Products", http://www/chromavision.com/products/index.htm, 2004.

Ciocca, et al., "Immunohistochemical Detection of an Estrogen-regulated Protein by Monoclonal Antibodies", *Cancer Research*, vol. 42, pp. 4256-4258, Oct. 1982.

Colcher, et al., "A spectrum of monoclonal antibodies reactive with human mammary tumor cells", *Proc. Natl. Acad. Sci.*, vol. 78, No. 5, pp. 3199-3203, May 1981.

Cote, et al., "Prediction of Early Relapse in Patients with Operable Breast Cancer by Detection of Occult Bone Marrow Micrometastases", *Journal of Clinical Oncology*, vol. 9, No. 10, pp. 1749-1756, Oct. 1991.

Cuttitta, et al., "Monoclonal antibodies that demonstrate specificity for several types of human lung cancer", *Proc. Natl. Acad. Sci.*, vol. 78, No. 7, pp. 4591-4595, Jul. 1981.

Diamond, et al., "Computerized Image Analysis of Nuclear Shape as a Prognostic Factor for Prostatic Cancer", *The Prostate*, vol. 3, pp. 321-332, 1982.

Diel, et al., "Monoclonal Antibodies to detect breast cancer cells in bone marrow", Accession No. 94266290, *Important Advances in Oncology*, pp. 143-164, 1994, Abstract.

Dippold, et al., "Cell surface antigens of human malignant melanoma: Definition of six antigenic systems with mouse monoclonal antibodies", *Proc. Natl. Acad. Sci.*, Vol. 77, No. 10, pp. 6114-6118, Oct. 1980.

Drobnjak, et al., "Immunocytochemical Detection of Estrogen and Progesterone Receptors (ER/PR) in Paraffin Sections of Human Breast Carcinoma, Correlation with Biochemical Analysis and Automated Imaging Quantitation", *Laboratory Investigation, a Journal of The United States and Canadian Academy of Pathology, Inc.*, Annual Meeting, Chicago, Illinois, Mar. 17-22, 1991.

Duda, et al., *Pattern Classification and Scene Analysis*, John Wiley & Sons, pp. 228-239; 276-284, 1973.

Enestrom, et al., "Quantitative Ultrastructural Immunocytochemistry Using a Computerized Image Analysis System", *Stain Technology*, vol. 65, No. 6, pp. 263-278, 1990.

Esteban, et al., "Quantification of Estrogen Receptors on Paraffin-Embedded Tumors by Image Analysis", *Modern Pathology*, vol. 4, No. 1, pp. 53-57, Jan. 1991.

Foster, et al., "Monoclonal Antibodies to the Human Mammary Gland", *Virchows Arch* (*Pathol. Anat.*), vol. 394, pp. 279-293, 1982.

Freedman, et al., "B-Cell Monoclonal Antibodies and Their Use in Clinical Oncology", Accession No. 91191374, *Cancer Investigation*, vol. 9, No. 1, pp. 69-84, 1991, Abstract.

Goldschrnidt, et al., "Automated lmmunohistochemical Estrogen Receptor Staining and Computerized Image Analysis-Comparison with Biochemical Methods".

Gong, et al., "Prostate-specific membrane antigen (PSMA)-specific monoclonal antibodies in the treatment of prostate and other cancers", Accession No. 2000312481, *Cancer and Metastasis Reviews*, vol. 18, No. 4, pp. 483-490, 1999, Abstract.

Greene, "Monoclonal Antibodies to human estrogen receptor", *Proc. Natl. Acad. Sci.*, vol. 77, No. 9, pp. 5115-5119, Sep. 1980.

Gross, et al., "Quantitative Immunocytochemistry of Hypothalamic and Pituitary Hormones", *The Journal of Histochemistry and Cythochemistry*, vol. 33, No. 1, pp. 11-20, 1985.

Hartelius K., et al. "Bayesian Grid Matching" Institute of Mathematical Modeling Technical University of Denmark (Nov. 22, 2000).

Herlyn, M., et al., "Colorectal carcinoma-specific antigen: Detection by means of monoclonal antibodies," *Proc. Natl. Acad. Sci.*, U.S.A., vol. 76, pp. 1438-1442, 1979.

Horsfall, D.J. et al., "Immunocytochemical assay for oestrogen receptor in fine needle aspirates of breast cancer by video image analysis", *Br. J. Cancer*, 59, 129-134, 1989.

Janeway, C.A., et al., "Immunobiology," The Immune System in Health and Disease *Current Biology Ltd.*, Garland Publishing Inc., pp. 2:3-2:5, 1994.

Kerns, B.J. et al., "Estrogen receptor status evaluated in formalin-fixed paraffin embedded breast carcinomas determined by automated immunohistochemistry and image analysis", *Proceedings of the American Association for Cancer Research*, vol. 35, Mar. 1994.

Kohler, C. et al., "Continuous cultures of fused cells secreting antibody of predefined specificity," *Nature*, vol. 256, pp. 495-497, 1975.

Kohler, C., et al., "Derivation of specific antibody-producing tissue culture and tumor lines by cell fusion," *Eur. J. Immunol.*, vol. 6, pp. 511-519, 1976.

Lastoria, S. et al., "Management of patients with ovarian cancer using monoclonal antibodies", Accession No. 93313141, *Biomedicine and Pharmacotherapy*, vol. 46, No. 10, pp. 453-63, 1992, Abstract.

Ledley, R.S. et al., "Fundamentals of True-Color Image Processing", *IEEE*, pp. 791-795, 1990.

Levine, Gary M. et al., "Quantitative Immunocytochemistry by Digital Image Analysis: Application to Toxicologic Pathology", *XICOLOGIC Pathology* ISSN:0192-6233, vol. 15, No. 3, pp. 303-307, 1987.

Lin, C.W. et al., Detection of exfoliated bladder cancer cells by monoclonal antibodies to tumor-associated cell surface antigens, Accession No. 91162409, *Journal of Occupational Medicine*, vol. 32, No. 9, pp. 910-916, Sep. 1990. Abstract.

Mansi, J.L., et al., "Bone Marrow Micrometastases in Primary Breast Cancer: Prognostic Significance After 6 Years' Follow-Up," *Eur. J: Cancer*, vol. 27, No. 12, pp. 1552-1555, 1991.

Martin, V. M., et al., "Immunomagnetic enrichment of disseminated epithelial tumor cells from peripheral blood by MACS," *Experimental Hematology*, vol. 26, pp. 252-264.(1998).

Maudelonde, T. et al., "Immunostaining of Cathepsin D in Breast Cancer: Quantification by Computerised Image Analysis and Correlation with Cytosolic Assay", *Eur. J. Cancer*, vol. 28A, No. 10, pp. 1686-1691, 1992.

McClelland, Richard A. et al., "Automated Quantitation of Immunocytochemically Localized Estrogen Receptors in Human Breast Cancer", Cancer Research 50, 3545-3550, Jun. 1990.

McClelland, Richard A., et al., "A Multicentre Study into the Reliability of Steroid Receptor Immunocytochemical Assay Quantification", *The European Journal of Cancer*, vol. 27, No. 6, pp. 711-715, Jun. 1991.

McGee, J O'D. et al., "A new marker for human cancer cells. 2. Immunohistochemical detection of the Ca antigen in human tissues with the Ca1 antibody," *The Lancet*, vol. 2, pp. 7-11, Jul. 3, 1982.

McKeough et al., "A Low-Cost Automatic Translation and Autofocusing System for a Microscope", *Measurement Science and Technology*, IOP Publishing, Bristol, GB, vol. 6, No. 5, pp. 583-587, May 1995.

Mize, R. Ranney et al., "Quantitative immunocytochemistry using an image analyzer. I. Hardware evaluation, image processing, and data analysis", *Journal of Neuroscience Methods*, vol. 26, pp. 1-24, 1988.

Moss, T.J., et al., "Prognostic Value of Immunocytologic Detection of Bone Marrow Metastases in Neuroblastoma," *The New England Journal of Medicine*, vol. 324, No. 4, pp. 219-226, Jan. 1991.

Nadler, L.M. et al., "A monoclonal antibody defining a lymphoma-associated antigen in man," J. Immunol., vol. 125, No. 2, pp. 570-577, 1980.

Naume, B., et al., "Immunomagnetic techniques for the enrichment and detection of isolated breast carcinoma cells in bone marrow and peripheral blood," *J. of Hematotherapy*, vol. 6, pp. 103-114, 1997.

Neame, P.B. et al., "The use of monoclonal antibodies and immune markers in the diagnosis, prognosis, and therapy of acute leukemia", Accession No. 94184108, *Transfusion Medicine Reviews*, vol. 8, No. 1, pp. 59-75, Jan. 1994. Abstract.

Neville, A.M., "Detection of tumor antigens with monoclonal antibodies", Accession No. 92096159, *Current Opinion in Immunology*, vol. 3, No. 5, pp. 674-678, Oct. 1991. Abstract.

Nuti, M. et al., "A monoclonal antibody (B72.3) defines patterns of distribution of a novel tumor-associated antigen in human mammary carcinoma cell populations", *Int. J. Cancer*, vol. 29, pp. 539-545, 1982.

Poynton, Frequently asked questions about color, www.inforamp.net/~poynton, pp. 1-24, Dec. 30, 1999.

Pratt, William K., *Digital Image Processing, 2nd Edition*, A Wiley-Interscience Publication, 1991.

Press, Michael F. et al., "Her-2/nue Expression in Node-negative Breast Cancer: Direct Tissue Quantitation by Computerized Image Analysis and Association of Overexpression with Increased Risk of Recurrent Disease", *Cancer Research*, vol. 53, pp. 4960-4970, Oct. 1993.

Price, J.O., et al., "Prenatal Diagnosis with Fetal Cells Isolated from Maternal Blood by Multiparameter Flow Cytometry," *AM. J. Obstet. Gynecol.*, vol. 165, pp. 1731-1737, Dec. 1991.

Price, M.R. et al., "Summary report on the ISOBM TD-4 Workshop: analysis of 56 monoclonal antibodies against the MUC1 mucin" Accession No. 1998084002, San Diego, CA, Nov. 17-23, 1996, *Tumour Biology*, vol. 19, Suppl. 1, pp. 1-20, 1998. Abstract.

Roca et al., "New Autofocusing Algorithm for Cytological Tissue in a Microscopy Environment", *Optical Engineering, Soc. of Photo-Optical Instrumentation Engineers*, Bellingham, US, vol. 37, No. 2, pp. 635-641, Feb. 1, 1998.

Russ, John C., *Image Processing Handbook, 2nd Edition*, Library of Congress Cataloging-in-Publication Data, 1995.

Scheinberg, D.A., "Monoclonal antibodies in the treatment of myelogenous leukemias", Accession No. 93199942, *Cancer Treat. and Res.*, vol. 64, pp. 213-232, 1993. Abstract.

Schultz, Daniel S., et al., "Comparison of Visual and CAS-200 Quantitation of Immunocytochemical Staining in Breast Carcinoma Samples", *Analytical and Quantitative Cytology and Histology*, vol. 14, No. 1, pp. 35-40, Feb. 1992.

Sell, S., "Cancer markers of the 1990s", Accession No. 90235478, *Clinics in Lab. Med.*, vol. 10, No. 1, pp. 1-37, Mar. 1990. Abstract.

Seregni, E. et al., "Mucinic tumor markers recognized by monoclonal antibodies", Accession No. 91217796, *J. Nuc. Med. and Allied Sci.*, vol. 34, No. 4, pp. 314-320, Oct.-Dec. 1990. Abstract.

Simpson, J.L. and Elias, S., "Isolating Fetal Cells From Maternal Blood—Advances in Prenatal Diagnosis Through Molecular Technology," *JAMA*, vol. 270, No. 19, pp. 2357-2361, Nov. 17, 1993.

Taylor-Papadimitriou, J. et al., "Monoclonal antibodies to epithelium-specific components of the human milk fat globule membrane: production and reaction with cells in culture," *Int. J. Cancer*, vol. 28, pp. 17-21, 1981.

Tyer, C.L., et al., "Breast cancer cells are effectively purged from peripheral blood progenitor cells with an immunomagnetic technique," *Clinical Cancer Research*, vol. 2, pp. 81-86, 1996.

Unnerstall, James R. et al., "New Approaches to Quantitative Neuropathology: Multtivariate Analysis of Morphologic and Neurochemical Measures", *Neurobiology of Aging*, vol. 8, pp. 567-569, Pergamon Journals Ltd., 1987.

Vaickus, L. et al., "Overview of monoclonal antibodies in the diagnosis and therapy of cancer", Accession No. 91322684, *Cancer Investigation*, vol. 9, No. 2, pp. 195-209, 1991. Abstract.

Vangsted, A.J., et al., "Monoclonal antibodies for diagnosis and potential therapy of small cell lung cancer—the ganglioside antigen fucosyl-GM1", Accession No. 94137489, *Acta Oncologica*, Vo 32, No. 7-8, pp. 845-851, 1993. Abstract.

Wallace, The JPEG Still Picture Compression Standard, IEEE Transactions on Consumer Electronics, vol. 38, No. 1, pp. xviii-xxxiv, Feb. 1992.

Wikstrand, C.J. and Bigner, D.C., "Expression of human fetal brain antigens by human tumors of neuroectodermal origin as defined by monoclonal antibodies," *Cancer Res.*, vol. 42, No. 1, pp. 267-275, Jan. 1982.

* cited by examiner

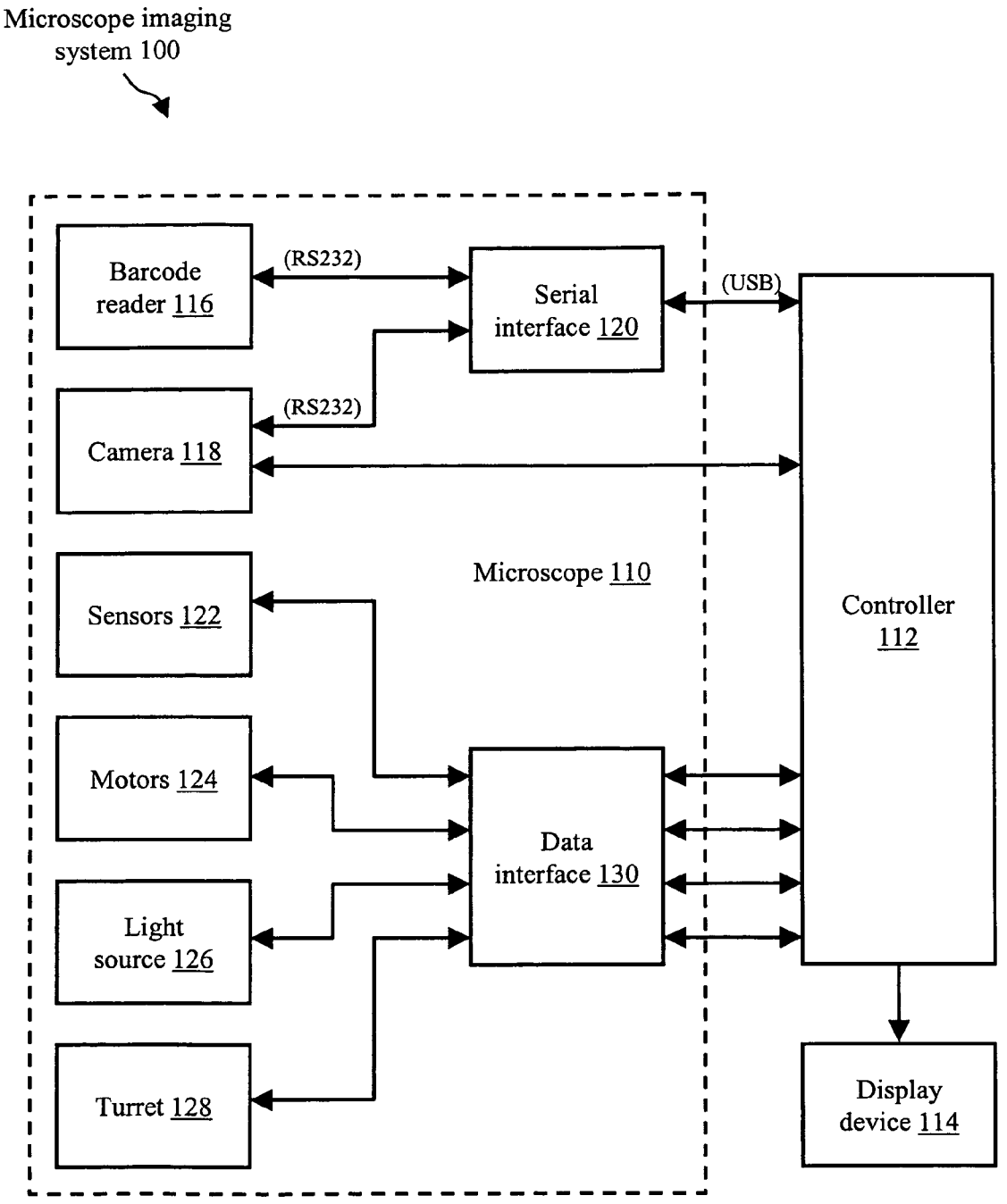
Microscope imaging system 100
Barcode reader 116
(RS232)
Serial interface 120
(USB)
(RS232)
Camera 118
Microscope 110
Sensors 122
Controller 112
Motors 124
Data interface 130
Light source 126
Turret 128
Display device 114

Fig. 1A

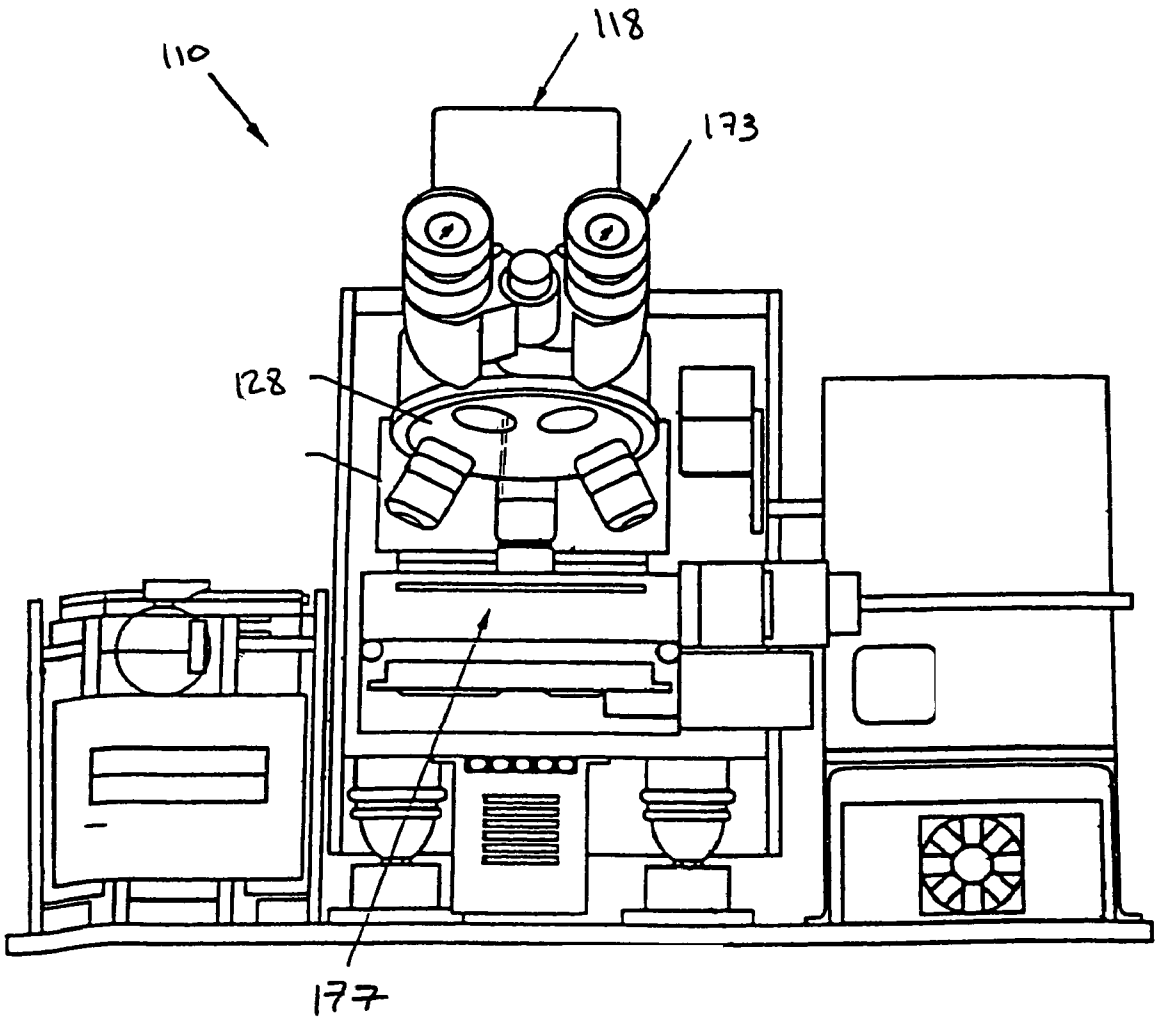

FIG. 1B

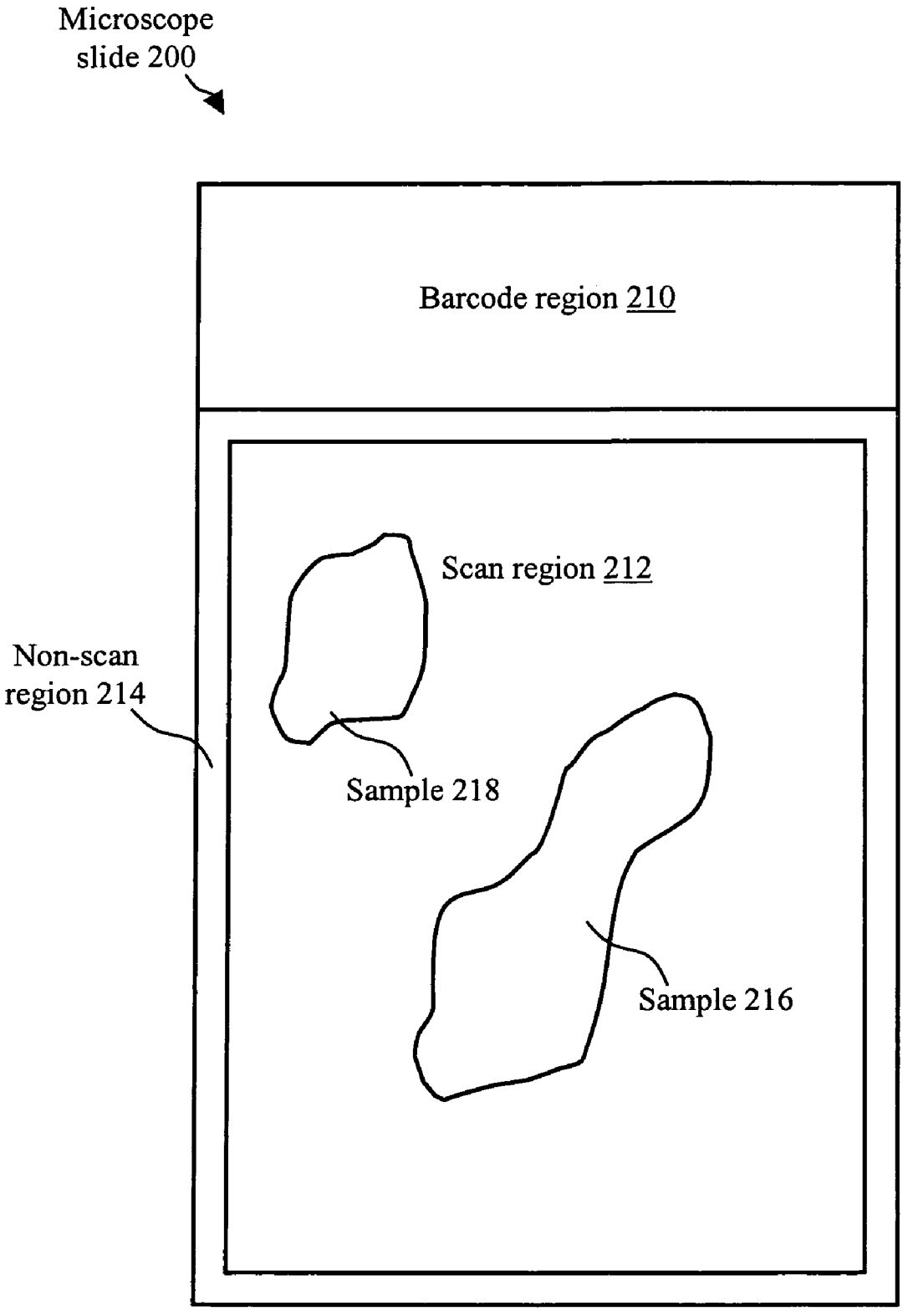
Microscope slide 200
Barcode region 210
Scan region 212
Non-scan region 214
Sample 218
Sample 216

Fig. 2

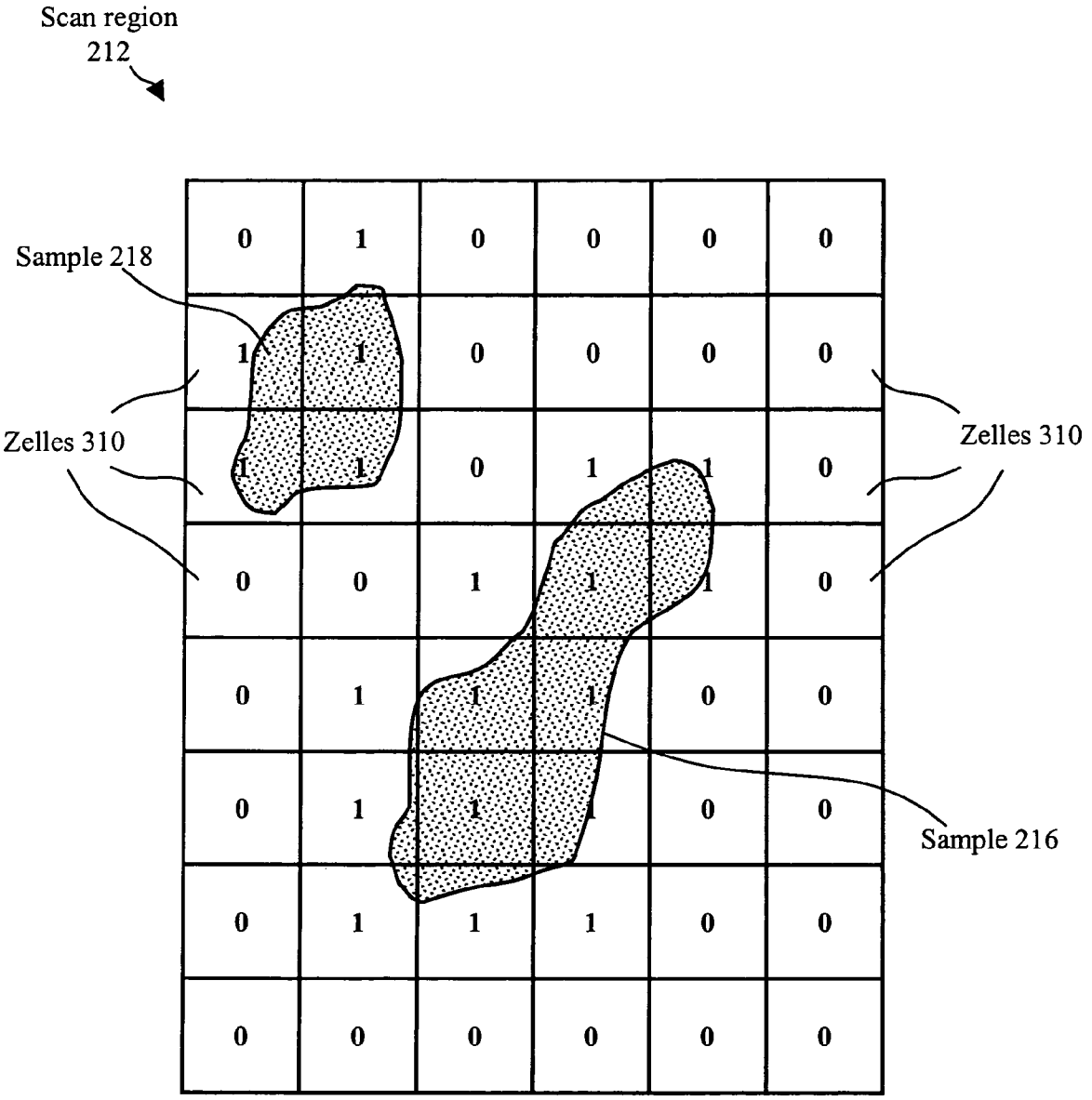
Scan region
212
Sample 218
Zelles 310
Zelles 310
Sample 216
0 1 0 0 0 0
1 1 0 0 0 0
1 1 0 1 1 0
0 0 1 1 1 0
0 1 1 1 0 0
0 1 1 1 0 0
0 1 1 1 0 0
0 0 0 0 0 0

Fig. 3

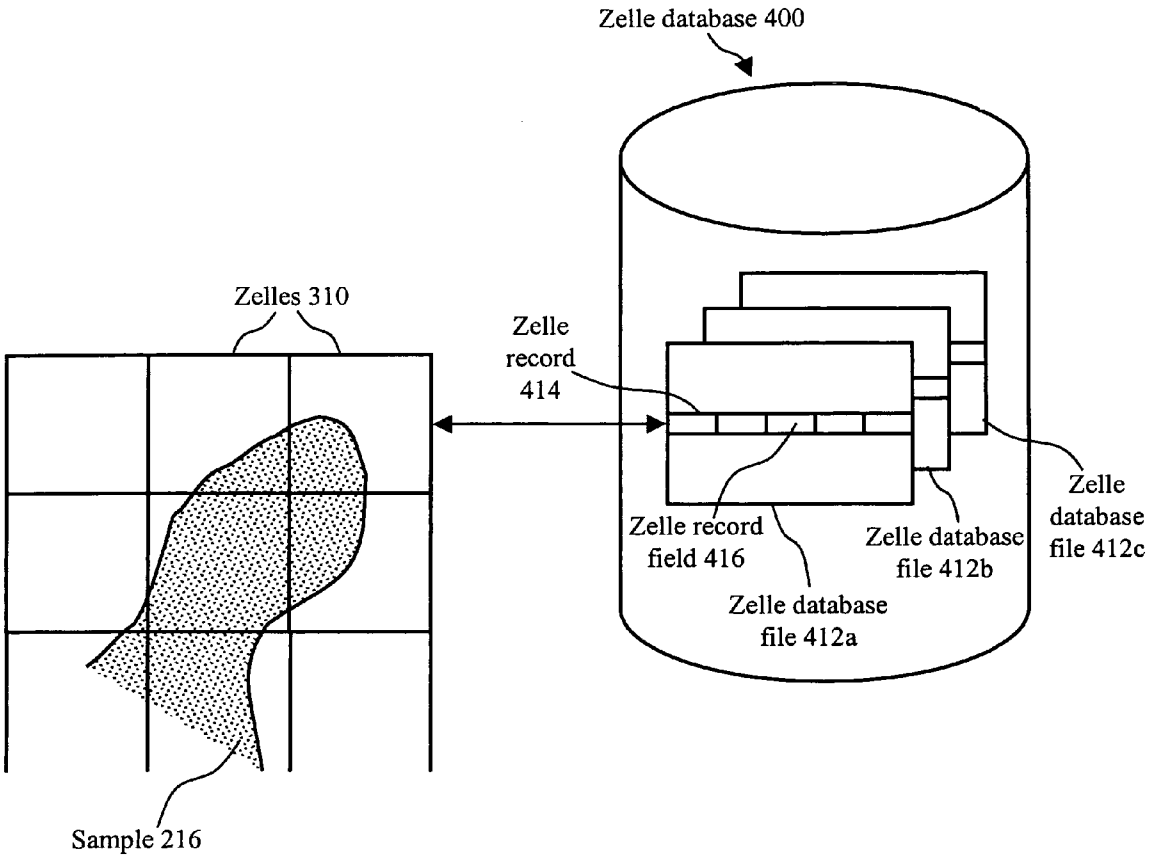
Zelle database 400
Zelles 310
Zelle record 414
Zelle record field 416
Zelle database file 412a
Zelle database file 412b
Zelle database file 412c
Sample 216

Fig. 4

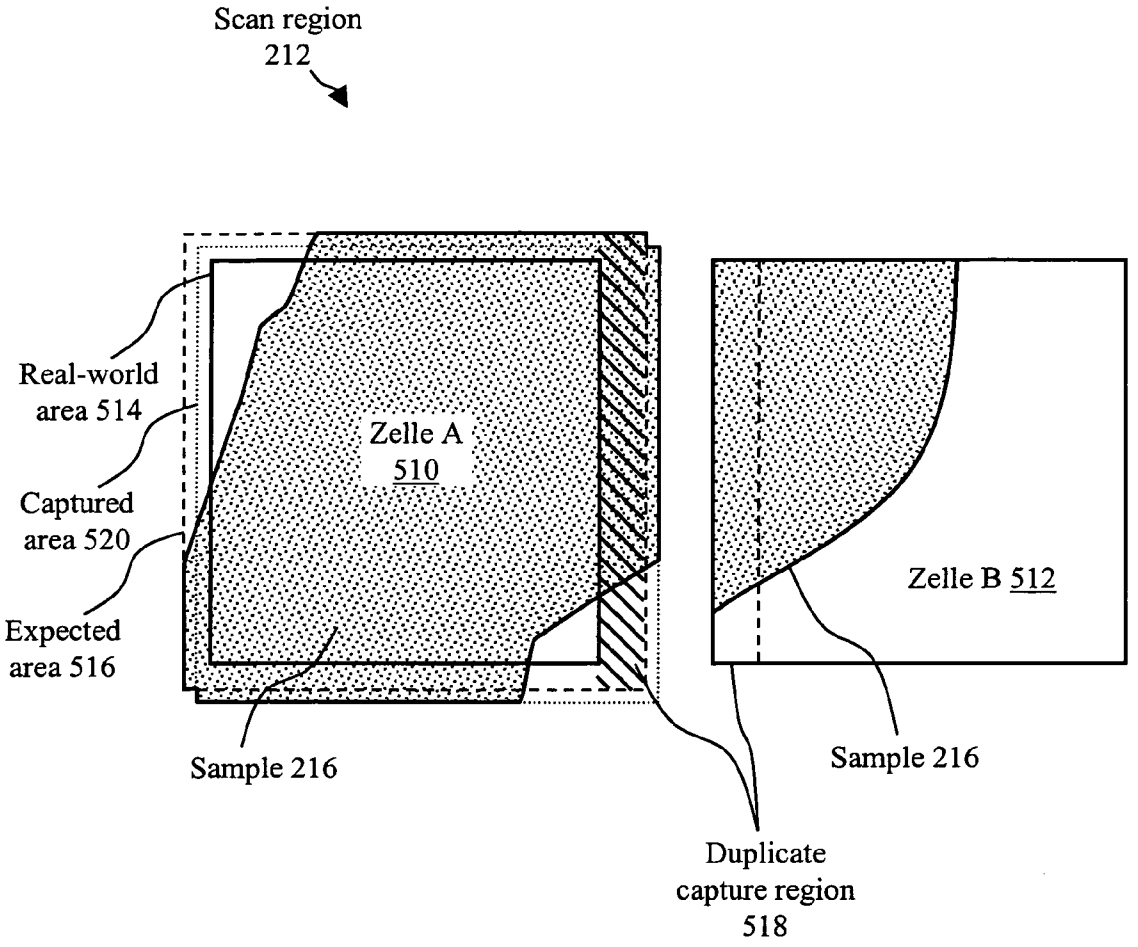
Scan region
212
Real-world
area 514
Captured
area 520
Expected
area 516
Zelle A
510
Zelle B 512
Sample 216
Sample 216
Duplicate
capture region
518

Fig. 5

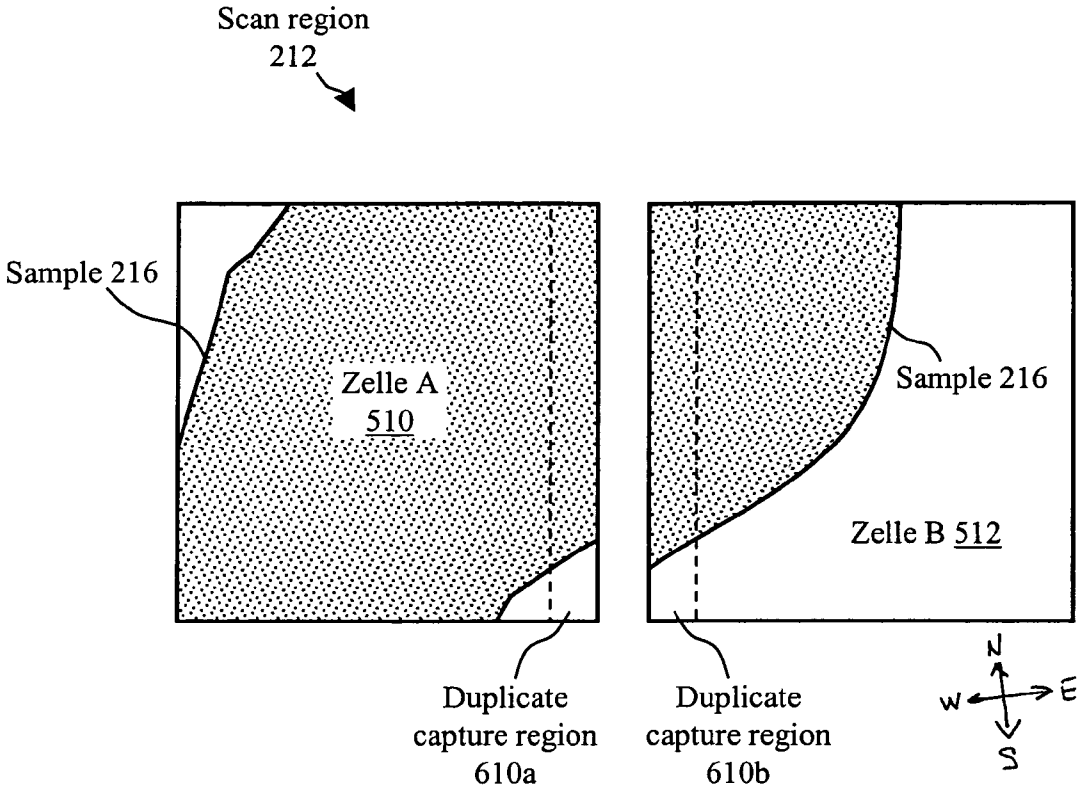
Scan region
212
Sample 216
Zelle A
510
Sample 216
Zelle B 512
Duplicate
capture region
610a
Duplicate
capture region
610b
N
W
E
S

Fig. 6A

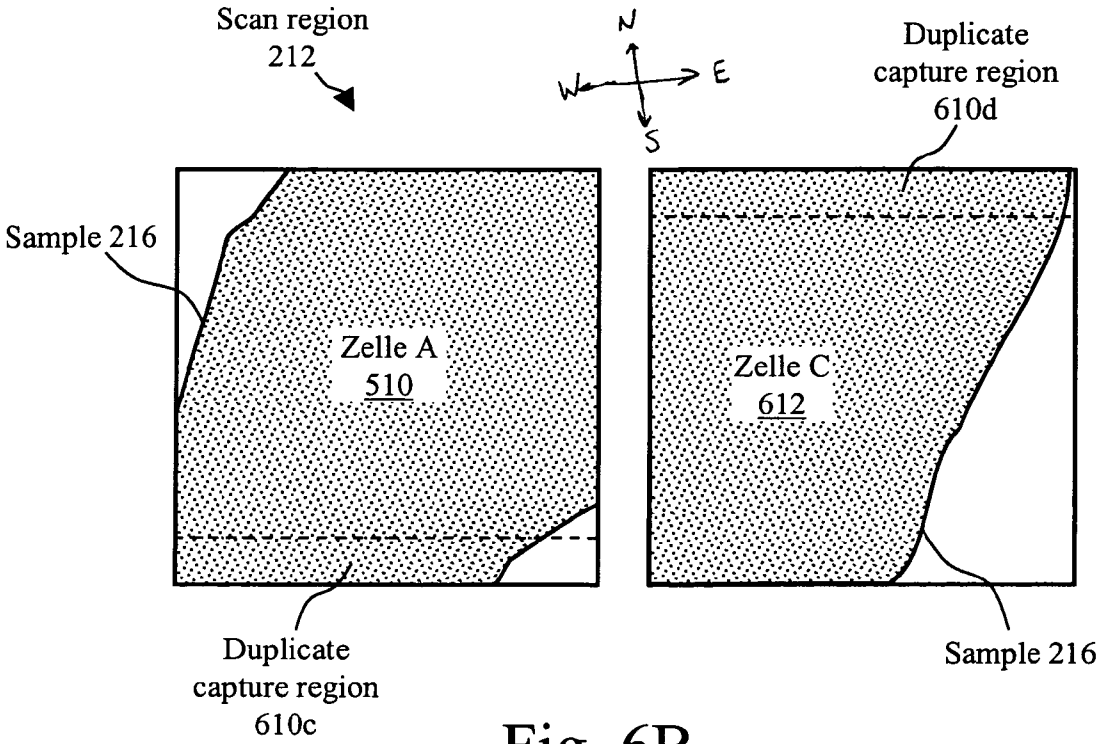
Scan region
212
N
W
E
S
Duplicate
capture region
610d
Sample 216
Zelle A
510
Zelle C
612
Duplicate
capture region
610c
Sample 216

Fig. 6B

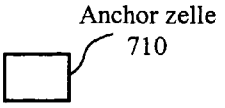

Fig. 7A

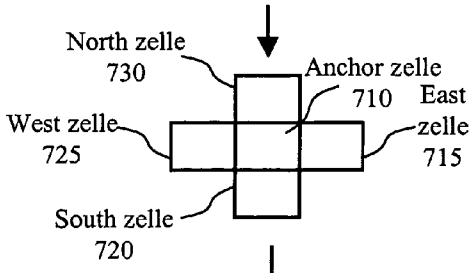

Fig. 7B

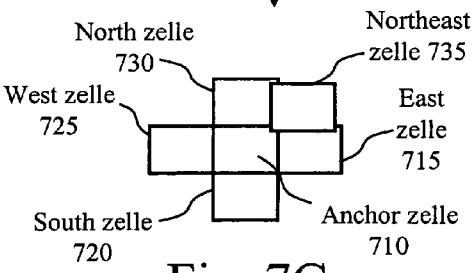

Fig. 7C

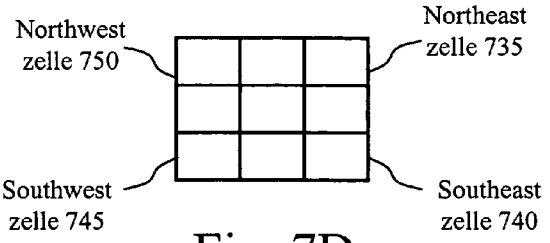

Fig. 7D

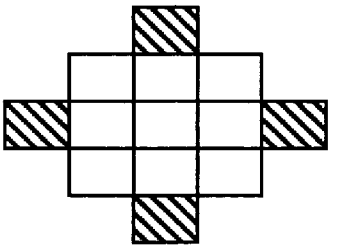

Fig. 7E

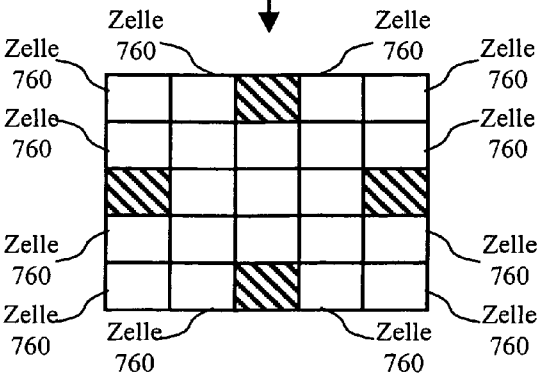

Fig. 7F

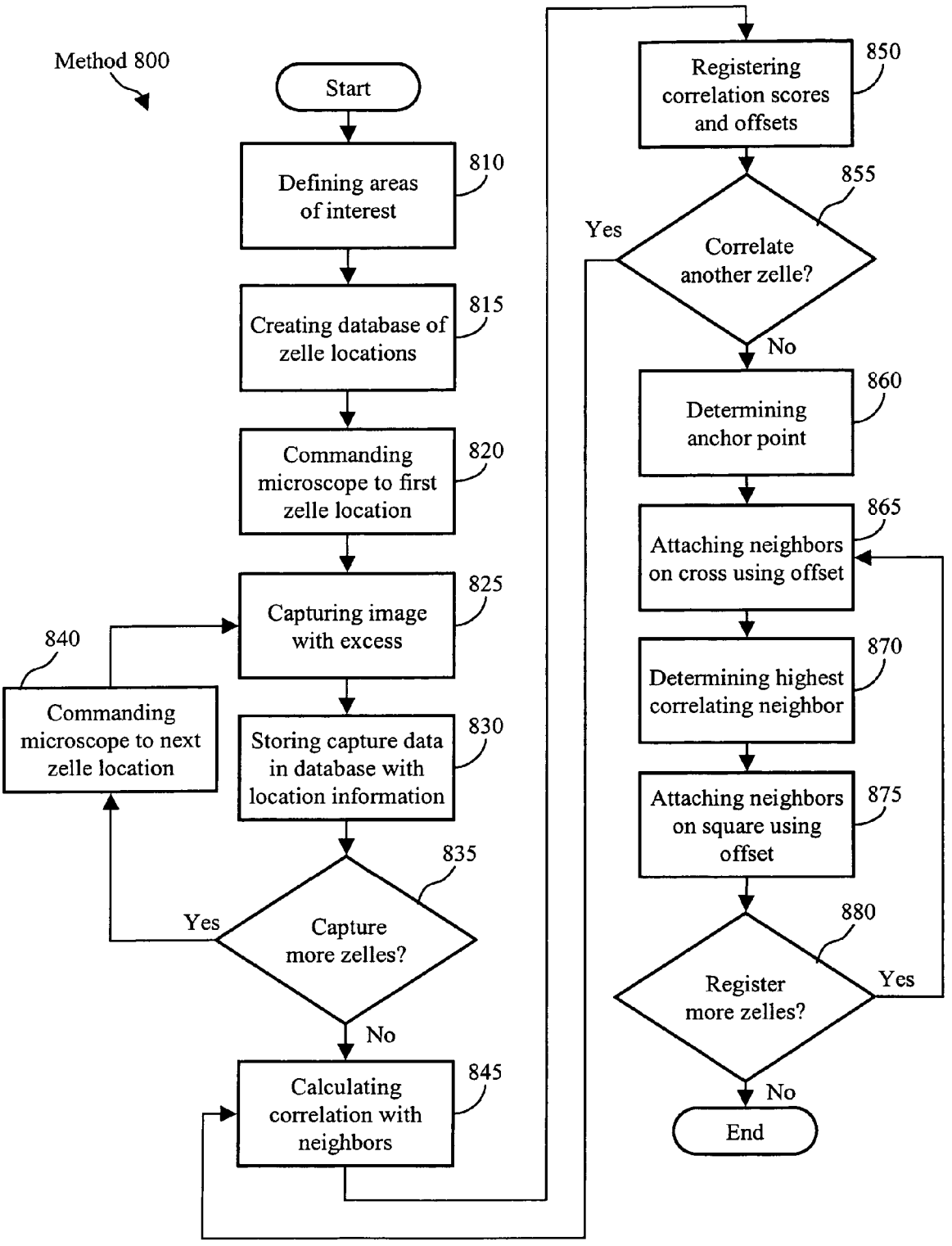
Method 800
Start
Defining areas of interest
810
Creating database of zelle locations
815
Commanding microscope to first zelle location
820
Capturing image with excess
825
Storing capture data in database with location information
830
Capture more zelles?
835
Yes
No
Commanding microscope to next zelle location
840
Calculating correlation with neighbors
845
Registering correlation scores and offsets
850
Correlate another zelle?
855
Yes
No
Determining anchor point
860
Attaching neighbors on cross using offset
865
Determining highest correlating neighbor
870
Attaching neighbors on square using offset
875
Register more zelles?
880
Yes
No
End

Fig. 8

SYSTEM AND METHOD OF REGISTERING FIELD OF VIEW

TECHNICAL FIELD

This disclosure relates to a system for and method of registering images captured by a computer-controlled microscope and, more particularly, this disclosure relates to optimizing the alignment of smaller fields of view captured by a computer-controlled automated microscope into larger fields of view.

BACKGROUND

In the field of anatomic pathology, a piece of human tissue is typically inspected and analyzed by marking a sample with a stain that reveals a visual indicator of diagnostic significance and then placing the stained tissue on a slide for viewing under a microscope. Automated imaging systems exist today that capture microscopic image data using a scanning instrument, such as a digital camera in combination with a computer-controlled microscope. Capturing areas of the slide sample at high magnification is necessary for examining minute features of the tissue. A single image of an entire tissue specimen at a high magnification such as 40× requires significant computer storage space and involves lengthy retrieval times. Alternatively, by collecting and storing the sample as any number of contiguous micro images at high objectives, the system can perform various compression techniques and make improvements to data acquisition, retrieval, display, and storage of the images.

A challenge relating to microscopy for anatomic pathology involves assembling micro images captured at high magnifications into a variety of fields of view. This could include a composite image of the entire slide sample or a field of view spanning any portion of the specimen. For example, U.S. Pat. No. 6,404,906, entitled, "Method and apparatus for acquiring and reconstructing magnified specimen images from a computer-controlled microscope," describes a method of using a computer-controlled microscope system to provide a reconstructed, seamless image from several contiguous fields of view to show the architecture and spatial relationship of biological material in a specimen. A macro image of contiguous image titles at a low magnification and optical resolution is obtained, and the user navigates within the macro image and selects areas. Higher magnification titles for the selected area are assembled and viewed at a higher magnification and optical resolution as a composite micro image of the selected area. Both the macro and micro images may be displayed simultaneously. Preferably, the user may scroll and cause additional fields of view to be added to previously displayed fields of view.

While the '906 patent provides a means of reconstructing micro images into other fields of view, it does not ensure that the system captured the expected image in the first place, nor does it explain what to do if image capture was imprecise. Calibration of such a system is frequently performed, but it is still unfeasible to account for every minor inaccuracy when working with images at very high magnification levels. One example of a calibration inaccuracy in the system might occur while moving the turret from one microscopic image to another. Because this process involves mechanical precision in measurements of microns, a slightly different image from what was expected may be captured. As a result, significant tissue samples may be overlooked. In addition, visible discontinuities may exist for any macro image including micro images where capture was inaccurate. What is needed is a means of seamlessly aligning microscopic images into larger fields of view.

Furthermore, if image capture by an automated microscope system is consistently inaccurate, this may indicate a need to calibrate the system. By analyzing the offset of each image, the system may be able to determine the variable by which inaccuracy is occurring. What is needed is a means of distinguishing between reasonable system inaccuracies and recurring system inaccuracies.

SUMMARY

Disclosed is a method of registering images captured by a computer controlled microscope. The method includes the steps of partitioning a microscopic image into a series of segments, wherein each segment comprises a discrete portion of the microscopic image; capturing image data for each of the segments, wherein the image data for each segment includes at least one duplicate region of image data that overlaps with the image data of an adjacent segment; determining an anchor segment by which all adjacent segments will be compared; and aligning the segments with one another to create a single macroscopic image comprised of the aligned segments. In one embodiment, the microscopic image relates to an image of a microscope slide having a biological sample and each segment is classified as either an interesting segment that contains at least a portion of the sample, or a nonintersecting segment that contains none of the sample.

For each segment, a correlation score is calculated indicative of the level of correlation of the segment with each of its adjacent segments. The correlation score is calculated by correlating the duplicate region of the segment to a corresponding duplicate region of an adjacent segment. Furthermore, at least one offset value is calculated relative to an adjacent segment. The offset value is indicative of the amount that the segment is offset relative to the adjacent segment. The correlation score and offset values are used to align adjacent segments to one another.

Also disclosed is a computer program on computer readable medium comprising instructions to cause a computer to partition a microscopic image into a series of segments, wherein each segment comprises a discrete portion of the microscopic image; capture image data for each of the segments, wherein the image data for each segment includes at least one duplicate region of image data that overlaps with the image data of an adjacent segment; determine an anchor segment by which all adjacent segments will be compared; and align the segments with one another to create a single macroscopic image comprised of the aligned segments.

Also disclosed is a microscope imaging system comprising a computer, which comprises a system processor and a computer program on computer readable medium. The computer program comprises instructions to cause the computer to partition a microscopic image into a series of segments, wherein each segment comprises a discrete portion of the microscopic image; capture image data for each of the segments, wherein the image data for each segment includes at least one duplicate region of image data that overlaps with the image data of an adjacent segment; determine an anchor segment by which all adjacent segments will be compared; and align the segments with one another to create a single macroscopic image comprised of the aligned segments.

The details of one or more embodiments of the invention are set forth in the accompanying drawings and the descrip-

tion below. Other features, objects, and advantages of the invention will be apparent from the description and drawings, and from the claims.

DESCRIPTION OF DRAWINGS

FIG. **1**A illustrates a high-level functional diagram of a microscope imaging system in accordance with the invention.

FIG. **1**B illustrates a front view of an exemplary microscope.

FIG. **2** illustrates a conventional microscope slide for use within the microscope imaging system.

FIG. **3** illustrates an expanded view of a scan region of the microscope slide during the automated image scanning operation.

FIG. **4** illustrates a relationship between each zelle and a zelle database that includes a plurality of database files, each containing a plurality of zelle records.

FIG. **5** illustrates a two adjacent zelles and shows both a minimum image area necessary for capture and an excess area that a microscope imaging system may capture.

FIGS. **6**A and **6**B illustrate a method of image correlation for two adjacent zelles.

FIGS. **7**A through **7**F illustrate a composite image of a series of zelles that is assembled by first determining an anchor zelle and then aligning each adjacent neighbor zelle using offsets and correlation calculations.

FIG. **8** illustrates a flow diagram of a method of capturing and registering microscopic images.

Like reference symbols in the various drawings indicate like elements.

DETAILED DESCRIPTION

Disclosed is a system for and a method of registering images captured by a computer-controlled microscope. The system and method can be used to capture a macro image of a tissue specimen, wherein the image is comprised collection of seamlessly-aligned microimages and wherein positioning inaccuracies that would prevent the omission of interesting sample image content are eliminated. The disclosed system and method also identifies possible calibration inaccuracies in an automated microscope system. In one aspect, the imaging system of the present invention divides a microscopic image into a plurality of regions, including interesting and non-interesting regions. Next, the system identifies only interesting regions of the microscopic image. The system then captures image data for each interesting region, wherein the image data for each region includes data that overlaps with an adjacent region. The system then determines an anchor region by which all adjacent regions will be compared. Each region is then aligned to create one seamless macroscopic image.

FIG. **1**A illustrates an exemplary high-level functional diagram of a microscope imaging system **100** configured in a manner that can be used to effect the disclosed systems and methods. The microscope imaging system **100** includes a microscope **110** electrically connected to a controller **112** having a display device **114**. The controller **112** in FIG. **1**A can be any special-purpose or conventional computer, such as a desktop, laptop, or host computer. The controller **112** is loaded with the appropriate software for controlling microscope imaging system **100**, such as software for running image-processing algorithms and image analysis algorithms. The display device **114** can be any special-purpose or conventional computer display device that outputs graphical images to a user.

In one embodiment, the microscope **110** is a computer-controlled microscope suitable for use in an automated imaging system. In one embodiment, the microscope **110** is a ChromaVision Automated Cellular Imaging System (ACIS). The microscope **110** further includes a barcode reader **116**, a camera **118**, a serial interface **120**, one or more sensors **122**, one or more motors **124**, a light source **126**, a turret **128**, and a data interface **130**, each of which is described further below.

The barcode reader **116** is a standard barcode reader capable of detecting an identifier located on, in the example of microscope imaging system **100**, a standard microscope slide, as described in more detail in reference to FIG. **2**. The barcode reader **116** can also comprise any type of device that can read and/or categorize an identifier located on the microscope slide.

The camera **118** can be a digital camera having selectable resolution capabilities. Furthermore, the camera can comprise any type of device suitable for gathering an image. The camera **118** is mounted upon a turret **128** of the microscope **110** such that an aperture of the camera **118** is aligned with the field of view (FOV) of any lens associated with the turret **128**. The barcode reader **116** and the camera **118** are electrically coupled to a serial interface such that they can feed electrical inputs to a serial interface **120**, which facilitates a serial communication link between the camera **118** and the barcode reader **116** and the controller **112**. In one embodiment, the serial interface **120** provides a USB connection to controller **112**. It should be appreciated that the camera **118** and the barcode reader **116** can be communicatively coupled to the controller **112** in other manners.

The controller **112** can include one or more components for facilitating its functions. In one embodiment, the controller includes a video card (not shown). The camera **118** provides a direct video output to the video card within the controller **112**. The video card gathers the image data from camera **118** for processing in a well-known manner.

With reference still to FIG. **1**A, the sensors can include one or more sensors for sensing various aspects of the imaging system **100**. For example, the sensors **122** include, but are not limited to, position sensors, temperature sensors, and light intensity sensors or optical encoders. The motors **124** can be any type of motors for providing motion to the microscope or any portion of the microscope. In one embodiment, the motors **124** are conventional servomotors associated with the motion control of microscope **110**, such as those for rotating the appropriately powered lens within the optical path of microscope **110**, for adjusting focus, or for controlling an automated X, Y stage (shown in FIG. **1**B).

The light source **126** can be any suitable light source for appropriately illuminating the FOV of microscope **110** sufficient to create a digital image of that FOV. The turret **128** is a conventional motor-driven microscope turret upon which is mounted a set of lenses of varying power that may be rotated into the optical path of the microscope **110**. The turret **128** is also suitably controlled to provide the desired focus. The sensors **122**, motors **124**, light source **126**, and turret **128** feed to the electrical inputs of the data interface **130**. The data interface **130** can be a conventional system driver card, which facilitates a data communication link between these elements and a motion control card (not shown) within the controller **112**.

FIG. **1**B shows a front view of an exemplary microscope **110**. A set of viewing oculars **173** of the microscope **110** are optionally located on the microscope **110** for operator viewing. As mentioned, the microscope **110** further includes a camera **118** for acquiring images. An automatic slide in-feed stage (not shown) in conjunction with an X-Y stage **177**

provide automatic slide handling in the apparatus. The illumination light source **126** (not shown in FIG. **1**B) projects light onto the X-Y stage **177**, which is subsequently imaged through the microscope **110** and acquired through the CCD camera **118** for processing in an image processor. A Z stage or focus stage **179** under control of the microscope controller **112** provides displacement in the Z plane for focusing. The microscope **110** further includes the motorized objective turret **128** for selection of objectives.

With reference now to FIGS. **1**A and **1**B, the generalized operation of microscope imaging system **100** is now described. In an initial operation, one or more standard microscope slides having at least one biological sample deposited thereon and stained with one or more chromogenic dyes is fed to the automated X-Y stage **177** of the microscope **110**. Each slide is fed via an in-feed stage (not shown) and subsequently is positioned in the FOV of microscope **110**. Additionally, as each slide transitions from the in-feed stage of the microscope imaging system **100** to the X, Y stage of the microscope **110**, an identifier of the target microscope slide is read by barcode reader **116** or is identified in another manner.

Once the slide is positioned in the FOV of the microscope **110**, an image scan operation is performed wherein the slide is scanned at a various resolutions and magnifications based upon image-processing algorithms and image analysis algorithms executed by the controller **112**. Upon completion of the image scan operation, the slide is transferred out of microscope imaging system **100** via an out-feed stage of the system. Furthermore, the slide ID and image data for that particular slide is transmitted to controller **112** and stored in memory. The motion control system then moves the next target slide into the FOV of the microscope **110**. The aforedescribed process automatically repeats for each microscope slide that is automatically fed into microscope imaging system **100**.

It should be appreciated that the microscope imaging system **100** can be configured to operate autonomously. That is, a clinician can initiate the microscope imaging system **100** such that the microscope imaging system **100** thereafter operates automatically without the need for human intervention as long as a supply of microscope slides is available at its in-feed stage and no system errors occur. At any time during the process, however, a clinician may view and/or manipulate the digital image of any given slide via controller **112** and display device **114** for the inspection and analysis of any given specimen, as is well known in anatomic pathology. This is possible because the controller **112** reconstructs the image using the image data associated with the contiguous FOVs and the image registration information. Alternately, the clinician and/or the controller can manually feed slides into the microscope imaging system.

With reference now to FIG. **2**, there is shown a conventional microscope slide **200** formed of any suitable material, such as, for example, glass, for use within microscope imaging system **100**. An identifier region **210** is located on the slide **200**, such as at one end of microscope slide **200**. A unique identifying tag is located in the identifier region **210**. The identifying tag can be, for example, a barcode sticker, or any tag that can be used to identify the slide **200**. The microscope slide **200** further includes a scan region **212**, which is at least partially surrounded by a non-scan region **214**. The scan region **212** represents a predetermined preliminary region of the slide **200** to be scanned. At least one sample, such as a sample **216** and a sample **218**, are likely to be entirely or partially located within the scan region **216**. The samples **216** and **218** are representative of any target specimen, such as, for example, a tissue sample resulting from a needle biopsy. The non-scan region **214** is the remaining area (excluding the scan region **216**) along the edge of the microscope slide **200**, within which it is unlikely that any sample is located. Consequently, the non-scan region **214** need not be scanned by the microscopic imaging system **100**.

FIG. **3** illustrates an expanded view of the scan region **212** of the microscope slide **200** during the automated scanning operation of the microscope imaging system **100**. The scan region **212** is partitioned into an array of contiguous segments, or zelles **310**. Each zelle **310** covers a discrete portion of the scan region **212** and all the zelles collectively cover the entire area of the scan region **212**. In one embodiment, the area of each zelle **310** is defined by the power (i.e., magnification) setting of the microscope **110**. Those skilled in the art will appreciate that a microscopic FOV reduces very substantially as the magnification increases.

In one embodiment, the zelles **310** are representative of the FOVs during an image scanning operation in which low magnification and resolution are used; thus, the scan time and the amount of stored image data is minimized. Additionally, a low-power lens has a greater depth of focus, so microscope **110** can search for tissue without the steps of refocusing. The low-power lens is focused at either a best-guess plane or a plane derived from microscope calibration during the image scanning operation. Optionally, a separate low-resolution, wide-FOV camera may be used.

The controller **112** executes image-processing algorithms and image analysis algorithms to determine any regions of microscope slide **200** having content worthwhile for re-examination at a higher magnification during later scanning phases. More specifically, the controller **112** classifies zelles containing specimen content in one category and classifies zelles containing no specimen content in a separate category. For example, any zelle **310** found to contain specimen content is classified as "interesting" and is mapped as a logical "1", as illustrated in FIG. **3**. By contrast, any zelle **310** found to have no specimen content is classified as "non-interesting" and is mapped as a logical "0." In this manner, a silhouette of each specimen, e.g., sample **216**, is collectively formed by the zelles **310**, thereby creating what is effectively a low-resolution image that may be processed using standard image-processing algorithms.

The parameters for analyzing each zelle **310** and determining whether there is anything of interest in each zelle **310** can be set by an operator depending on the test and application. In this way, the operator can vary how a zelle **310** will be classified. In order to efficiently perform the analysis of the zelles **310**, it is desirable to avoid analyzing empty zelles **310** (i.e., zelles with no specimen content) so as to avoid unnecessarily using processing power and time of the controller **112**. At the same time, there is a need to ensure that the controller does not miss any zelle **310** having mostly empty space and only a tiny segment of interest, but rather classifies such zelles as "interesting". For example, the lower, left edge (with respect to FIG. **3**) of the sample **216** is partially located within a zelle and it is desirable that this zelle not be missed. Thus, a statistical algorithm is run to determine whether there is anything of interest in each zelle **310** in order to reduce the likelihood of missing any zelles with sample located therein.

The manner in which a zelle is classified as "interesting" can be unique and varied to each particular application or test. For example, a priority may be set for blue stain, red stain, any speck of tissue, or a specified large volume of tissue in order for a zelle **310** to be classified as "interesting." Consequently, the biological requirements of each particular test, as set by an operator, determine what is of interest and determine the parameters for classifying a zelle as "interesting." Therefore, each zelle **310** is analyzed using predetermined parameters

for a particular test using associated algorithms that determine whether what is found in each zelle **310** matches the predetermined criteria. If what is found in a particular zelle meets the predetermined criteria, then that zelle is classified as "interesting."

With reference to FIG. **4**, the zelles **310** derived from a particular sample can be stored in a database. FIG. **4** illustrates the relationship between each zelle **310** derived from, for example, the sample **216** and a zelle database **400**. In one embodiment, the zelle database **400** is a non-volatile computer memory that resides on a physical hard drive (not shown) of the controller **112** of microscope imaging system **100**. The zelle database **400** contains a plurality of zelle database files **412** (e.g., zelle database files **412***a*, **412***b*, and **412***c* in FIG. **4**), wherein each zelle database file **412** contains one or more zelle records **414**. Each zelle record **414** further includes a plurality of record fields **416** composed of binary digital data (not shown). In one embodiment, each zelle record **414** contains multiple zelle record fields **416** that each describe one or more individual attributes of its respective associated zelles **310**. The attributes can vary and can include, for example, an identification number of scanned microscope slide **200**, scale factors, the area of zelle **310**, the time and date of the scan operation, the identification number of microscope imaging system **100**, an image file address where the image data record for zelle **310** is stored, and a pointer to the image data record within the image file. Other useful information may also be contained in the database.

The zelle database **400** also includes placeholders for the width and height coordinates of each zelle **310**. The width and height coordinates can be with respect to a coordinate system, such as a Cartesian coordinate system comprised of x and y coordinates that are oriented relative to a reference point on the slide. The process of capturing and inserting these coordinates into the zelle database **400** is referred to as the "registration" process. The registration process of these coordinates can occur either during the image capture process (referred to as "online") or after the image capture process is complete (referred to as "offline"). Ideally, each pair of adjacent zelles **310**, as defined by their width and height coordinates, should align contiguously with one another if microscope **110** captures each zelle as partitioned in FIG. **3**. However, due to the nature of automated microscope **110** taking images at very high magnifications, minor inaccuracies during image capture may occur. Therefore, the zelles **310** can be captured with overlapping coverage areas to make sure that no region of an image is missed due to mechanical inaccuracies in the microscope **110**.

FIG. **5** illustrates a first step in the aforementioned registration process. FIG. **5** shows a zelle A **510** from sample **216**, which is adjacent to a zelle B **512** on the slide **200**. During the process of partitioning an entire image into zelles **310** (as described above with respect to FIG. **3**), the coordinates of the area of each zelle **310** as it relates to its real-world coordinates on the physical slide are identified and captured, creating a real-world area **514**. For example, if the microscope slide **200** has real-world coordinates that range between 0 and 600 microns in width (x) and between 0 and 800 microns in height (y), the zelle A **510** within microscope slide **200** may have real-world coordinates x ranging, for example, between 400 and 500 microns in width and real world coordinates y ranging between 400 and 500 microns in height, given where zelle A **510** exists and how the zelle images have been partitioned within the scan region **212**. The zelle B **512**, which is considered a "neighbor" because it is adjacent to the right of zelle A **510**, may have real-world coordinates ranging between 500 and 600 microns in width and the same 400 to 500 microns in height as zelle A **510**, given that it sits directly to the right of zelle A **510** (with respect to FIG. **5**).

As mentioned, for each zelle **310**, the microscope **110** captures more image data than is truly necessary in order to compensate for the aforementioned inaccuracies with such a system. Because the system knows the real-world area **514** of the zelle A **510**, the system can calculate an overlap or duplicate capture area for each side of zelle A **510**, thus making sure that no region is missed. A duplicate capture region **518** in FIG. **5** is an example of the overlap area between neighboring zelle A **510** and zelle B **512**.

The size of the duplicate capture region **518** can vary. For example, the duplicate capture region might be an extra 20 microns in width to the right of zelle A **510** and an extra 20 microns in width to the left of zelle B **512**. Once the size of the duplicate capture region is determined, the system has the area that microscope **110** is commanded to capture. This is shown in FIG. **5** as an expected area **516**, which includes the real-world area **514**, the duplicate capture region **518**, and any other additional capture regions for each side of zelle A **510**. Therefore, the microscope **110** might be commanded to scan zelle A **510** at a width ranging between 380 and 520 microns and a height that might also range between 380 and 520 microns, which includes the real world width and height of the zelle A **510** plus an allowance for any duplicate capture regions. This additional capture is done for all zelles **310**.

Although the microscope **110** may have been commanded to capture the expected area **516**, minor inaccuracies may have caused the system to capture a slightly different image, shown as a captured area **520** in FIG. **5**, which can include just a portion of the expected area **516**. In fact, such inaccuracies may occur for any or all zelles **310**; however, because inaccuracies occur within extra capture areas of each zelle image, the system does not miss key image data. That is, the duplicate capture regions of the zelles ensure that the system does not miss key data as a result of minor inaccuracies in the system. However, given that the expected area **516** and the captured area **520** may be different, the system may no longer understand the true coordinates of real-world area **514** as they relate to captured area **520**.

FIGS. **6**A and **6**B illustrate how a correlation algorithm is used to solve this problem by deriving an offset between each pair of adjacent zelles **310**, wherein the offset comprises the distance by which the area of each zelle should be adjusted in order to properly align the zelles. For each of a zelle **310**'s neighbors to the east (E), west (W), north (N) and south (S) (with reference to the legend shown in FIGS. **6**A and **6**B), a duplicate capture region **518** is captured as described above with reference to FIG. **5**. A standard, two-dimensional cross-correlation algorithm compares the areas of overlap between each pair of zelles **310** to determine how much the images are offset. Those skilled in the art will appreciate that, knowing a priori the intended area of overlap, the algorithm needs only to be run on this area and not run over the entirety of both images. The areas of the two duplicate capture regions **518** may be sized differently to ensure that common imagery of one zelle **310** is within the other zelle **310**.

As an example, in FIG. **6**A, a duplicate capture region **610***a* of zelle A **510** is compared with a duplicate capture region **610***b* of zelle B **512**. In FIG. **6**B, a duplicate capture region **610***c* of zelle A **510** is compared with a duplicate capture region **610***d* of a zelle C **612** using the same correlation algorithm. As a result of correlation, each zelle **310** is matched with all of its neighbors, resulting in up to four offset values for each zelle, which are stored in zelle database **400**.

In addition to storing offset values, a correlation score between each pair of adjacent zelles **310** is calculated and

stored, wherein the correlation score is indicative of how well the duplicate capture regions of a pair of adjacent zelles correlate to one another. For example, due to the extra white space in duplicate capture region **610***c* when compared with duplicate capture region **610***d* (shown in FIG. **6**B), it appears that the algorithm will estimate a lower correlation score between zelle A **510** and zelle C **612**, possibly as low as, for example, 75%. Therefore, between these two neighbors, zelle B **512** may have a higher correlation score with zelle A **510** than zelle C **612** does. This score is used during a second registration process when a single zelle **310** has conflicting offset values between two of its neighbors, which is described further in reference to FIG. **7**C.

In one embodiment, the correlation algorithm has a list of at least three displacements between neighbors that are not allowed such that any neighbors violating the list do not receive a passing correlations score. These include displacements in which two neighboring zelles **310** overlap too little across X, overlap too much across X, or overlap too much across Y. Any neighbors violating such displacements do not receive a passing correlation score, even if they have a high match of offsets. Additional displacement calculations can always be used within the algorithm, and adjustments can be made to any of the allowed displacement values.

FIGS. **7**A through **7**F illustrate the second registration step that is performed. The second registration step occurs after image data has been captured and stored as described in FIG. **5** and offsets and correlation scores between each pair of zelles **310** have been calculated and stored as described in FIG. **6**. At this point, the microscope imaging system **100** can perform a registration process that creates one contiguous image.

FIG. **7**A illustrates that microscope imaging system **100** first determines a good starting point for deciding how to piece the image together. This starting point is known as an anchor zelle **710**. To determine anchor zelle **710**, an algorithm is run to determine the most "connected" zelle **310**. The most "connected" zelle is the zelle that has the greatest number of adjacent neighbor zelles **310** with sample content to the north, south, east, and/or west. If a zelle **310** has four adjacent neighbor zelles **310**, this zelle **310** is referred to as being "four-connected". If one or more zelles **310** have an equally high number of connections, the algorithm then determines which is closest to the center of the image. These two factors determine which single zelle **310** is known as anchor zelle **710**. The anchor zelle **710** could also be calculated using any other parameters. Because inaccuracies tend to build upon themselves, starting with an anchor point at a corner of the image and reconstructing the image in a raster-like pattern is not as accurate as starting with a central anchor and building the image outwards. Thus, it can be desirable for the anchor zelle to be as close to the center of the image as possible.

To register anchor zelle **710**, the microscope imaging system **100** sets the original real-world area of anchor zelle **710** as the actual registered area and stores the coordinates in zelle database **400**. For example, if zelle A **510** is determined to be the most appropriate anchor zelle **710**, real-world area **514** becomes the registered area for zelle A **510**.

FIG. **7**B illustrates the next process of, "attaching on cross" wherein neighboring zelles to the east, west, north and south (with respect to FIG. **7**B) are aligned contiguously with the anchor zelle. By setting the registered positions of an east zelle **715**, a south zelle **720**, a west zelle **725**, and a north zelle **730** according to the derived offsets each had with anchor zelle **710**, as calculated by the correlation algorithm illustrated in FIG. **6**, these four neighbors are aligned contiguously with anchor zelle **710**.

FIG. **7**C illustrates the next process of "attaching on square" wherein zelles diagonal (i.e., northeast, northwest, southeast, and southwest) to the anchor zelle are aligned thereto. Unlike the process of attaching on cross, a northeast zelle **735** could potentially have matching offsets with both east zelle **715** and north zelle **730**. To remedy this, the previously-calculated correlation score is used to determine which offset to use. The pair that has the highest correlation score is used in matching offsets.

FIG. **7**D shows northeast zelle **735**, a southeast zelle **740**, a southwest zelle **745**, and a northwest zelle **750** aligning contiguously with previously registered east zelle **715**, south zelle **720**, west zelle **725**, and north zelle **730**, having performed "attaching on square" as described in reference to FIG. **7**C. FIG. **7**E shows that the process of "attaching on cross" is repeated, as four additional zelles **310** to the east, south, west, and north are registered relative to their neighbor zelles. It can be seen in FIG. **7**E that thirteen zelles have now been aligned. The process of comparing the offsets and correlation scores of neighboring zelles is successively performed until all relevant zelles have been continuously aligned. For example, FIG. **7**F shoes that the process of "attaching on square" is repeated. However, the process now compares correlation scores for determining offsets for twelve new neighbor zelles **760**—three each to the northeast, southeast, southwest, and northwest. The registration process continues until all zelles **310** are registered and attached to the contiguous image.

FIG. **8** illustrates a flow diagram of a method **800** of the entire process of capturing and registering microscopic images in accordance with the invention. The controller **112** can perform the process pursuant to instructions on a computer-readable medium. In a first operation, represented by the flow diagram box **810** in FIG. **8**, the areas of interest on the slide **200** are defined. Pursuant to this step, the microscope imaging system **100** scans the microscope slide **200** at a low resolution to identify where content (such as sample **216** and sample **218** in FIG. **2**) exists on the slide. The system partitions the entire image into a series of smaller segments of images called zelles **310**, such as shown in FIG. **3** and described above.

The process then proceed to the operation represented by the flow diagram box **815**, where a database of zelle locations is created. The coordinates of a real-world area, (such as real-world area **514** for zelle A **510** shown in FIG. **5**) are logged in a zelle database **400**, such as shown and described above with reference to FIG. **4**. The coordinates are known because the system previously partitioned the image into these zelles **310** in the operation represented by flow diagram box **810**.

The process then proceeds to the operation represented by the flow diagram box **820**. Pursuant to this operation, the microscope imaging system **100** is commanded to move the FOV to the first zelle location. As discussed above, the imaging system **100** is equipped with motors **124** that can be used to move the FOV to a desired location. Once the microscope imaging system **100** is moved to the first zelle location, the process proceeds to the step represented by the flow diagram box **825**, where the image is captured with excess area, as was described above with reference to FIG. **5**. Specifically, the microscope imaging system **100** captures an image of a zelle **310**, such as the zelle A **510** (FIG. **5**) at a high resolution. This captured image includes excess image data for each side of zelle **310**, wherein the excess image data comprises the previously-described duplicate capture region **518**, for example.

In the next operation, the relevant data relating the zelle is captured in a database that includes location information for

the zelle, as represented by the flow diagram box **830** in FIG. **8**. The image data and coordinates of the captured area, such as the captured area **520** for zelle A **510**, are logged in the zelle database **400**, as shown and described above with respect to FIG. **4**. As discussed, this captured area may be slightly larger or smaller than the expected area, e.g., expected area **516**, depending on inaccuracies experienced within microscope imaging system **100**.

The process then proceeds to the operation represented by the flow diagram decision box **835**, where it is determined whether more zelles need to be captured in order to capture the entire sample or samples on the slide **200** at high resolution. If more zelles indeed need to be captured (a "yes" output from the decision box **835**), the process proceeds to the operation represented by flow diagram box **840**. In the operation **840**, the microscope imaging system **100** is commanded to move to the next zelle location. The process then returns to the operation of flow diagram box **825**.

However, if no more zelles need to be captured, the process proceeds to the operation represented by flow diagram box **845**. Pursuant to this operation, the correlation of the neighboring zelles is calculated in the manner described above. Each zelle **310** is correlated with at least one of its neighbors containing sample content on the slide. As mentioned, a correlation algorithm is performed using duplicate capture regions between two zelles **310** to obtain a correlation score for each zelle relative to all if its neighbors. For example, the duplicate capture regions **610***a* and **610***b* between zelle A **510** and zelle B **512** (shown in FIG. **6**A), respectively, can be correlated. The process then proceeds to the operation represented by flow diagram box **850**, where the correlation scores and offsets for the zelle are registered and stored. In this operation, the offsets and correlation score of each pair of neighboring zelles **310** are stored within the zelle database **400**.

In the next operation, represented by the flow diagram decision box **855**, it is determined whether another zelle needs to be correlated with at least one neighbor. If another zelle needs to be correlated (a "yes" output from decision box **855**), the process returns to the operation of flow diagram box **845** where the correlation process repeats for the next zelle.

If no other zelles need to be correlated (a "no" output from the flow diagram box **855**), then the process proceeds to the operation represented by flow diagram box **860**. Pursuant to this operation, the anchor point is determined. As discussed above, the anchor point, such as an anchor zelle, is the starting point for piecing together the resultant macro image. The anchor zelle is the zelle by which all adjacent regions will be compared in the initial operation. As discussed above, the anchor point is determined using a calculation of connectedness and centrality for each zelle. The real-world coordinates of the anchor point are logged as its registered coordinates in the zelle database **400**. For example, the coordinates of the real-world area **514** of zelle A **510** become its registered coordinates.

The process then proceeds to the operation represented by the flow diagram box **865**. Pursuant to this operation, neighboring zelles that are adjacent to the east, west, north and south are attached "on cross" using the previously-calculated offset, as was described above with reference to FIG. **7**B. Each neighbor of the anchor zelle **710**, such as the east zelle **715** in FIG. **7**B, is registered by comparing the offset of each neighbor versus the registered coordinates of the anchor zelle **710**. This operation effectively attaches the neighbor zelle contiguously with the anchor zelle.

The process next proceeds to the operation of flow diagram box **870**, where the highest correlated neighbor is determined for the anchor zelle (or whatever zelles is currently being processed). Each neighbor zelle **310** of the current zelle (such as east zelle **715**, which neighbors zelle **710** in FIG. **7**C), that was attached on cross in the operation of flow diagram box **865** may have adjacent zelles **310** that also need registration. For example, the northeast zelle **735** and southeast zelle **740** in FIG. **7**C may also need registration. However, the neighbor zelles **310** can have conflicting offsets. For example, the northeast zelle **735** has an offset with both east zelle **715** and north zelle **730**. Consequently, the highest correlating neighbor is determined by using correlation calculations from the operation of flow diagram box **845**.

The process then proceeds to the next operation, represented by flow diagram box **875**. In this operation, neighbor zelles are attached to the current zelle "on square" using the previously-calculated offsets. In this step, each adjacent zelle **310**, such as northeast zelle **735** in FIGS. **7**C and **7**D, is registered by comparing the offset between it and its highest correlating neighbor (as determined in step **870**). This effectively attaches the adjacent zelle **310** contiguously with the anchor zelle and neighbors on cross by storing its registered coordinates.

In the next operation, represented by the flow diagram decision box **880** in FIG. **8**, it is determined whether more zelles need to be registered. If more zelles indeed need to be registered (a "yes" output from decision box **865**), then the process returns to the operation of flow diagram box **865**, where the neighboring zelles are registered and attached. If no more zelles need to be registered (a "no" output from decision box **880**), then the process ends.

A number of embodiments of the invention have been described. Nevertheless, it will be understood that various modifications may be made without departing from the spirit and scope of the invention. Accordingly, other embodiments are within the scope of the following claims.

What is claimed is:

1. A computer implemented method of registering images captured by a computer controlled microscope, comprising:

partitioning a microscope image of a microscope slide having a biological sample into a series of segments, wherein each segment comprises a discrete portion of the microscopic image;

classifying each segment as either an interesting segment that contains at least a portion of the sample or a non-interesting segment that contains none of the sample;

capturing image data for each of the segments, wherein the image data for each segment includes at least one duplicate region of image data that overlaps with the image data of an adjacent segment;

determining an anchor segment by which all adjacent segments will be compared, wherein the anchor segment is determined based on which segment has the highest number of adjacent interesting segments; and

aligning the segments with one another to create a single macroscopic image comprised of the aligned segments.

2. A method as defined in claim **1**, wherein the capturing, determining, and aligning steps are performed only on segments classified as interesting.

3. A method as defined in claim **1**, further comprising storing attribute data relative to each segment in a database.

4. A method as defined in claim **3**, wherein the attribute data include the area covered by each segment as defined by a coordinate system.

5. A method as defined in claim **1**, further comprising, for each segment, calculating at least one correlation score indicative of the level of correlation of a segment with each of its adjacent segments, wherein the correlation score is calcu-

lated by correlating the duplicate region of the segment to a corresponding duplicate region of an adjacent segment.

6. A method as defined in claim **5**, further comprising, for each segment, calculating at least one offset value relative to an adjacent segment, the offset value being indicative of the amount that the segment is offset relative to the adjacent segment.

7. A method as defined in claim **6**, wherein aligning the segments with one another comprises:

using the offset values of each of the anchor zelle's adjacent segments to contiguously align each of the adjacent segments to the anchor zelle; and

using the correlation scores to resolve conflicting offset values between the adjacent segments and the anchor segment, wherein the offset value corresponding to the neighbor with the highest correlation score relative to the anchor segment is used to align the neighbor segments to the anchor segment.

8. A method as defined in claim **7**, further comprising successively aligning all of the segments to the anchor segment to form the single macroscopic image.

9. A method as defined in claim **8**, wherein a north, south, east or west adjacent segment is aligned to a subject segment prior to aligning a diagonal segment to the subject segment.

10. A method as defined in claim **1**, wherein the anchor segment is further determined based on which segment is closest to the center of the microscopic image.

11. A computer program on computer readable medium comprising instructions to cause a computer to:

partition a microscopic image into a series of segments, wherein each segment comprises a discrete portion of the microscopic image;

classify each segment as either an interesting segment that contains at least a portion of the sample or a non-interesting segment that contains none of the sample;

capture image data for each of the segments, wherein the image data for each segment includes at least one duplicate region of image data that overlaps with the image data of an adjacent segment;

determine an anchor segment by which all adjacent segments will be compared, wherein the anchor segment is determined based on which segment has the highest number of adjacent interesting segments; and

align the segments with one another to create a single macroscopic image comprised of the aligned segments.

12. A computer program as defined in claim **11**, wherein the instructions further cause the computer to:

for each segment, calculate at least one correlation score indicative of the level of correlation of a segment with each of its adjacent segments, wherein the correlation score is calculated by correlating the duplicate region of the segment to a corresponding duplicate region of an adjacent segment.

13. A computer program as defined in claim **12**, wherein the instructions further cause the computer to:

for each segment, calculate at least one offset value relative to an adjacent segment, the offset value being indicative of the amount that the segment is offset relative to the adjacent segment.

14. A computer program as defined in claim **13**, wherein the instructions further cause the computer to:

use the offset values of each of the anchor zelle's adjacent segments to contiguously align each of the adjacent segments to the anchor zelle; and

use the correlation scores to resolve conflicting offset values between the adjacent segments and the anchor segment, wherein the offset value corresponding to the neighbor with the highest correlation score relative to the anchor segment is used to align the neighbor segments to the anchor segment.

15. A computer program as defined in claim **13**, wherein the instructions further cause the computer to successively align all of the segments to the anchor segment to form the single macroscopic image.

16. A computer program as defined in claim **11**, wherein the anchor segment is further determined based on which segment is closest to the center of the microscopic image.

17. A microscopic imaging system comprising:

a computer comprising:

a system processor;

a computer program on computer readable medium, the computer program comprising instructions to cause the computer to:

partition a microscopic image into a series of segments, wherein each segment comprises a discrete portion of the microscopic image;

classify each segment as either an interesting segment that contains at least a portion of the sample or a non-interesting segment that contains none of the sample;

capture image data for each of the segments, wherein the image data for each segment includes at least one duplicate region of image data that overlaps with the image data of an adjacent segment;

determine an anchor segment by which all adjacent segments will be compared, wherein the anchor segment is determined based on which segment has the highest number of adjacent interesting segments; and

align the segments with one another to create a single macroscopic image comprised of the aligned segments.

18. A system as defined in claim **17**, wherein the instructions further cause the computer to:

for each segment, calculate at least one correlation score indicative of the level of correlation of a segment with each of its adjacent segments, wherein the correlation score is calculated by correlating the duplicate region of the segment to a corresponding duplicate region of an adjacent segment.

19. A system as defined in claim **18**, wherein the instructions further cause the computer to:

for each segment, calculate at least one offset value relative to an adjacent segment, the offset value being indicative of the amount that the segment is offset relative to the adjacent segment.

20. A system as defined in claim **19**, wherein the instructions further cause the computer to:

use the offset values of each of the anchor zelle's adjacent segments to contiguously align each of the adjacent segments to the anchor zelle; and

use the correlation scores to resolve conflicting offset values between the adjacent segments and the anchor segment, wherein the offset value corresponding to the neighbor with the highest correlation score relative to the anchor segment is used to align the neighbor segments to the anchor segment.

21. A system as defined in claim **19**, wherein the instructions further cause the computer to successively align all of the segments to the anchor segment to form the single macroscopic image.

22. A system as defined in claim **17**, wherein the anchor segment is further determined based on which segment is closest to the center of the microscopic image.

* * * * *